



Synthesis and growth mechanism of SiC/SiO₂ nanochains by catalyst-free thermal evaporation method in Ar/CO atmosphere

Xiang-min XIE¹, Zhe-an SU¹, Dong HUANG², Cheng YANG¹,
Ya-feng WANG¹, Ding-yu JIANG¹, Qi-zhong HUANG¹

1. National Key Laboratory of Science and Technology for National Defence on High-strength Structural Materials,
Central South University, Changsha 410083, China;

2. Hunan Provincial Engineering Research Center for High Performance Pitch Based Carbon Materials,
Hunan Toyi Carbon Material Technology Co., Ltd., Changsha 410205, China

Received 10 January 2020; accepted 10 July 2020

Abstract: SiC/SiO₂ nanochains were synthesized on a carbon fiber substrate by a catalyst-free thermal evaporation method in the Ar/CO atmosphere. X-ray diffraction (XRD), Fourier-transform infrared spectroscopy (FT-IR), scanning electron microscopy (SEM) and transmission electron microscopy (TEM) revealed that the as-synthesized SiC/SiO₂ nanochains are composed of single-crystalline SiC nanowires and amorphous SiO₂ beads. The introduction of CO can promote the formation of SiO₂, so that the SiC/SiO₂ nanochains are subsequently formed during cooling. In addition, the photoluminescence spectrum of SiC/SiO₂ nanochains showed a broad emission peak at around 350 nm, which is ascribed to the oxygen discrepancy in the SiO₂ beads as well as the SiC/SiO₂ interfacial effect. These findings can provide guidance for further study of the vapor growth of 1D SiC-based materials.

Key words: synthesis; growth mechanism; SiC/SiO₂ nanochains; thermal evaporation method; carbon monoxide; photoluminescence properties

1 Introduction

Silicon carbide (SiC) is an important material which is widely applied in nuclear industry, aerospace, and semiconductor [1–4]. The SiC nanowires have, in particular, demonstrated that they are good candidates for making functional optoelectronic devices thanks to their large band gap, as well as the quantum confinement effect when their crystallite size is reduced to nanoscale [5]. Various technologies such as pyrolysis of precursor [6], chemical vapor deposition [7,8], microwave heating [9] and carbothermal reduction [10,11] enable us to

precisely fabricate SiC nanowires. However, most of these methods involve metal catalyst which is difficult to be removed and may affect properties of nanowires [6,12], so the catalyst-free thermal evaporation method is now widely accepted for the fabrication of SiC nanowires [13,14].

The SiC nanowires which are coated with SiO₂ beads, are called SiC/SiO₂ nanochains [15–18]. These SiC/SiO₂ nanochains exhibit the enhanced electronic properties due to the SiC/SiO₂ interfacial effect, which is a great advantage in the application for functional materials [19]. LI et al [20] synthesized SiC/SiO₂ nanochains via molten salt-mediated chemical vapor reaction technique, and suggested that the SiO₂ beads can effectively

Foundation item: Project (U19A2088) supported by the National Natural Science Foundation of China; Project (2019RS2058) supported by the Special Fund for Innovative Construction of Hunan Province, China

Corresponding author: Zhe-an SU; Tel: +86-13873188002; E-mail: suza@csu.edu.cn

DOI: 10.1016/S1003-6326(20)65442-5

enhance the photoluminescence properties of the SiC/SiO₂ nanochains. It was proposed that the controllable and predictable fabrication of SiO₂ can broaden the application of SiC/SiO₂ nanochains greatly [21,22]. As a result, many researchers have investigated the growth mechanisms of SiC/SiO₂ nanochains. For instance, HOU et al [15] synthesized SiC/SiO_x nanochains via polymer-pyrolysis process, and found that the reactant concentration played a crucial role in controlling the final morphology of SiO₂. CHU et al [23] synthesized SiC/SiO₂ nanochains with different morphologies at different temperatures, and they ascribed this kind of results to the differences in both the SiO partial pressure and the Plateau-Rayleigh instability. Carbon monoxide (CO) is a common reductant, which is closely related to the carbothermal reduction synthesis of metal oxide nanostructures [24–26]. Similarly, it is assumed that CO can also affect the formation mechanism of SiO₂ nanostructures during the vapor growth of SiC nanowires, but no effort has been made so far to verify this assumption experimentally.

In this work, SiC/SiO₂ nanochains were synthesized by a catalyst-free thermal evaporation method in the Ar/CO atmosphere at 1400 °C. The comparative experiments conducted in the Ar atmosphere enable us to understand the effect of CO on the vapor growth of SiO₂, and determine the formation mechanism of the SiC/SiO₂ nanochains. In addition, the photoluminescence properties of the SiC/SiO₂ nanochains were also characterized, which may be served as a reference for the application in the field of optoelectronic device.

2 Experimental

2.1 Synthesis of SiC/SiO₂ nanochains

Figure 1 illustrates the experimental setup for the preparation of SiC/SiO₂ nanochains. The silicon powder purchased from Tianjin Kernel Chemical Reagent Co., Ltd., was used as the silicon source, and the carbon fiber purchased from Toray Industries, Inc. was used as both the carbon source and the substrate. Firstly, 5 g of silicon powder was added into a graphite crucible, and a carbon fiber with a length of 5 cm was fixed on the top of the silicon powder. Secondly, the graphite crucible was placed into an electric resistance furnace. After

being evacuated to about 100 Pa by a vacuum pump, the furnace was filled with Ar (99.99%) until total pressure reached 0.11 MPa. Thirdly, the furnace was heated until the temperature reached 1400 °C with CO (99.99%) being introduced into the furnace for a dwell time of 5 h. The flow rates of Ar and CO were 1 and 0.3 L/min, respectively. Finally, the furnace was cooled down naturally in the Ar atmosphere, and the white cotton-like nanostructures were obtained on the carbon fiber substrate. A comparative experiment was also performed by the same procedure but without introducing CO.

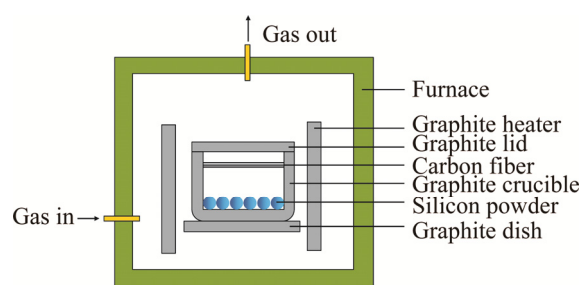


Fig. 1 Experimental setup for fabricating SiC/SiO₂ nanochains

2.2 Characterization

The morphologies of the products were investigated using scanning electron microscopy (SEM, FEI Quanta 250 FEG). The crystalline phase measurements were carried out using X-ray diffraction (XRD, Rigaku Dmax/2550 18 kW) from a Cu K_α source with a wavelength λ of 0.1542 nm. The surface functional groups were identified using Fourier-transform infrared spectroscopy (FT-IR, Thermo Fisher Scientific). The microstructures were characterized by transmission electron microscopy (TEM, FEI, Titan G2 60–300) including high-resolution transmission electron microscopy (HRTEM). The room temperature photoluminescence (PL) emissions were recorded using a fluorescence spectrophotometer (Hitachi F-7000, Xe lamp).

3 Results and discussion

3.1 Morphologies and microstructures of SiC nanowires and SiC/SiO₂ nanochains

Figure 2 shows the SEM images of the products synthesized in different atmospheres. Figures 2(a) and (b) display that a large number of

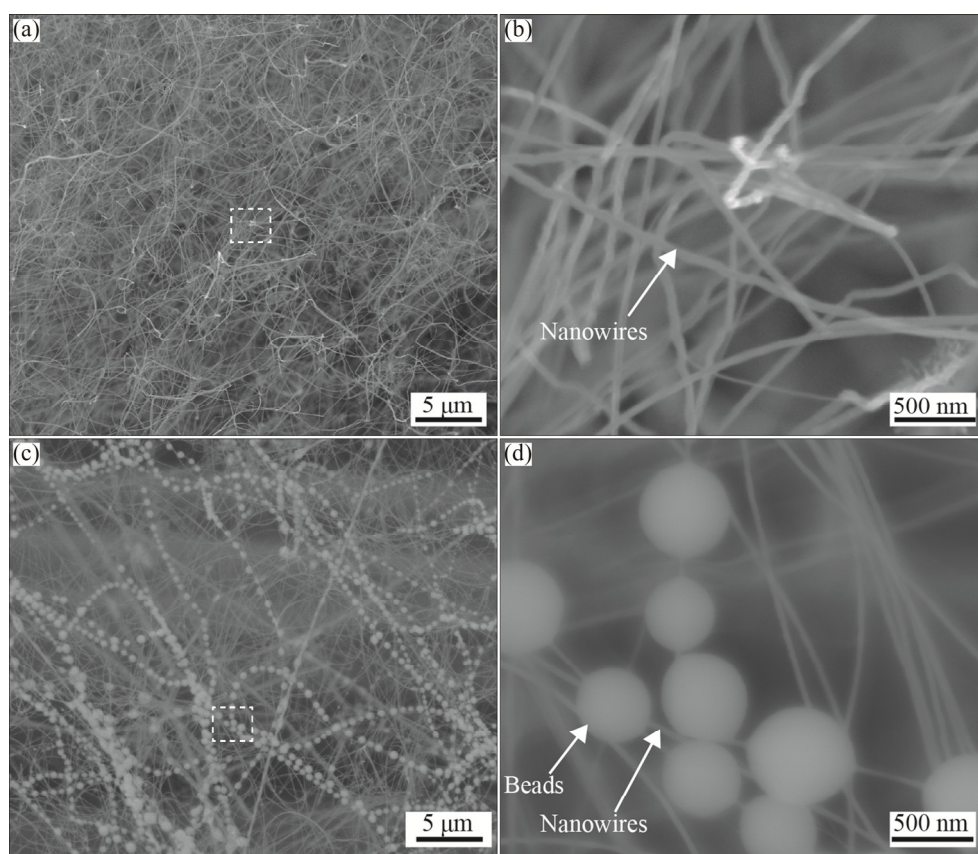


Fig. 2 SEM images of products synthesized under different atmospheres: (a, b) Low and high magnification SEM images of nanowires synthesized in Ar atmosphere, respectively; (c, d) Low and high magnification SEM images of nanostructures synthesized in Ar/CO atmosphere, respectively

entangled and uniform nanowires are formed after vapor growth in the Ar atmosphere. Their diameters are in a range of 30–60 nm and their lengths are hundreds of micrometers. Other nanostructures such as beads have not been detected. By contrast, the nanochains are formed after vapor growth in the Ar/CO atmosphere (Fig. 2(c)). The lengths of the nanochains are about several tens of micrometers. Figure 2(d) further reveals that the nanochains mainly consist of beads and nanowires. The periodic beads display a smooth surface with a diameter range of 300–600 nm, and they are strung together by the nanowires with a diameter in the range of 30–60 nm. It is inferred that the introduction of CO can induce the formation of periodic beads on nanowires during vapor growth and thus affect the final morphology of the 1D nanostructures.

To determine the crystalline phase and surface functional groups of the 1D nanostructures, X-ray diffraction and FT-IR spectroscopy analyses were performed. Figure 3 displays the XRD patterns of

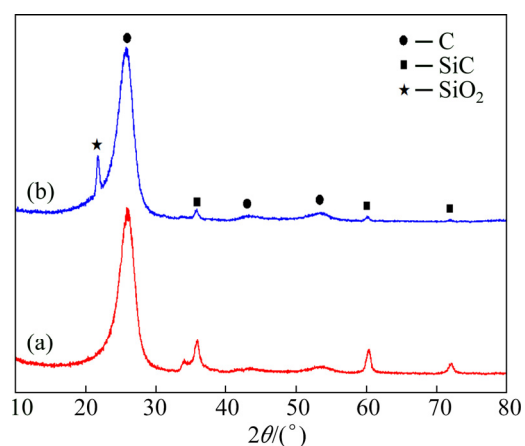


Fig. 3 XRD patterns of products synthesized in different atmospheres: (a) Ar; (b) Ar/CO

the products obtained in the Ar atmosphere (Fig. 3(a)) and the Ar/CO atmosphere (Fig. 3(b)), respectively. A strong diffraction peak at 2θ value of 25.8° is associated with the (002) crystal plane of graphite (JCPDS No. 75-1621), which is derived from the carbon phase of the fiber substrate. In addition, three diffraction peaks at 2θ values of

35.8°, 60.3° and 72.1° match the (111), (220) and (311) planes of the cubic SiC (JCPDS No. 29-1129), respectively. Interestingly, a sharp peak at 2θ value of 21.7° appears in Fig. 3(b), which is indexed to the crystal structure of the SiO₂ (JCPDS No. 39-1425). Figure 4 presents the FT-IR spectra of the products obtained in the Ar atmosphere (Fig. 4(a)) and the Ar/CO atmosphere (Fig. 4(b)). A sharp peak at around 797 cm⁻¹ is observed (Fig. 4(a)), corresponding to the Si—C stretching vibration band [27]. Besides, two other absorption peaks can be seen at around 1101 and 478 cm⁻¹ (Fig. 4(b)), which can be ascribed to the Si—O—Si stretching band [28]. Combined with the XRD results, it can be inferred that the main product synthesized in the Ar atmosphere is SiC, whereas the main products synthesized in the Ar/CO atmosphere are SiC and SiO₂, suggesting that the introduction of CO can induce the formation of SiO₂.

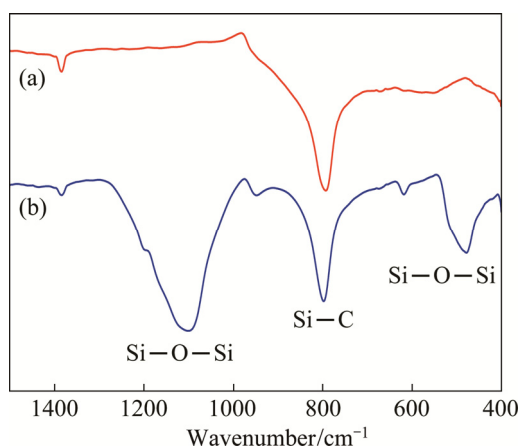


Fig. 4 FT-IR spectra of products synthesized in different atmospheres: (a) Ar; (b) Ar/CO

TEM examinations including the HRTEM were conducted to acquire the microstructural information of the 1D nanostructures. Figure 5(a) illustrates the TEM image of a typical SiC nanowire synthesized in the Ar atmosphere, which has a diameter of 35 nm and grows along the axial direction. The spacing between two lattice planes along the growth direction is 0.25 nm (Fig. 5(b)), indicating that the nanowire has a cubic SiC structure, but no other crystalline or amorphous structures can be observed. The growth mechanism of high purity SiC nanowires formed in the Ar atmosphere can be explained as follows. Firstly, both the silicon powder and the graphite crucible

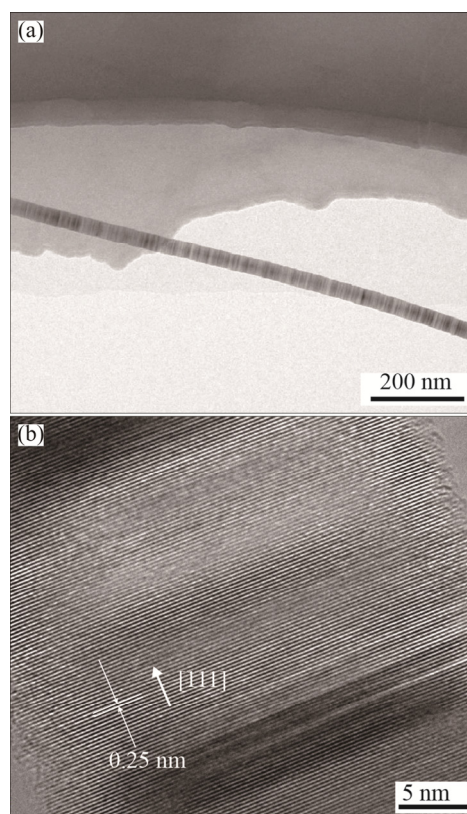


Fig. 5 TEM (a) and HRTEM (b) images of nanowire synthesized in Ar atmosphere

can react with O₂ to generate SiO and CO gases at the synthesis temperature, as described in Eqs. (1) and (2) (the residual O₂ is believed to come from the residual air at 100 Pa in the furnace and the impurity of the Ar [29,30]). Subsequently, the formed SiO will react with C and CO on the carbon fiber according to Eqs. (3) and (4), and thus generates the SiC nanowires. This oxide-assisted mechanism for the fabrication of SiC nanowires has also been reported by some other researchers [31,32].

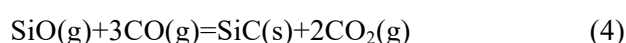


Figure 6 shows the TEM images of SiC/SiO₂ nanochain synthesized in the Ar/CO atmosphere. To better observe and study the microstructure of SiC/SiO₂ nanochain, we divide it into two parts: a bead and a string. The bead (Fig. 6(a)) possesses a smooth surface and its diameter is about 350 nm. HRTEM image (Fig. 6(b)) clearly shows the lattice

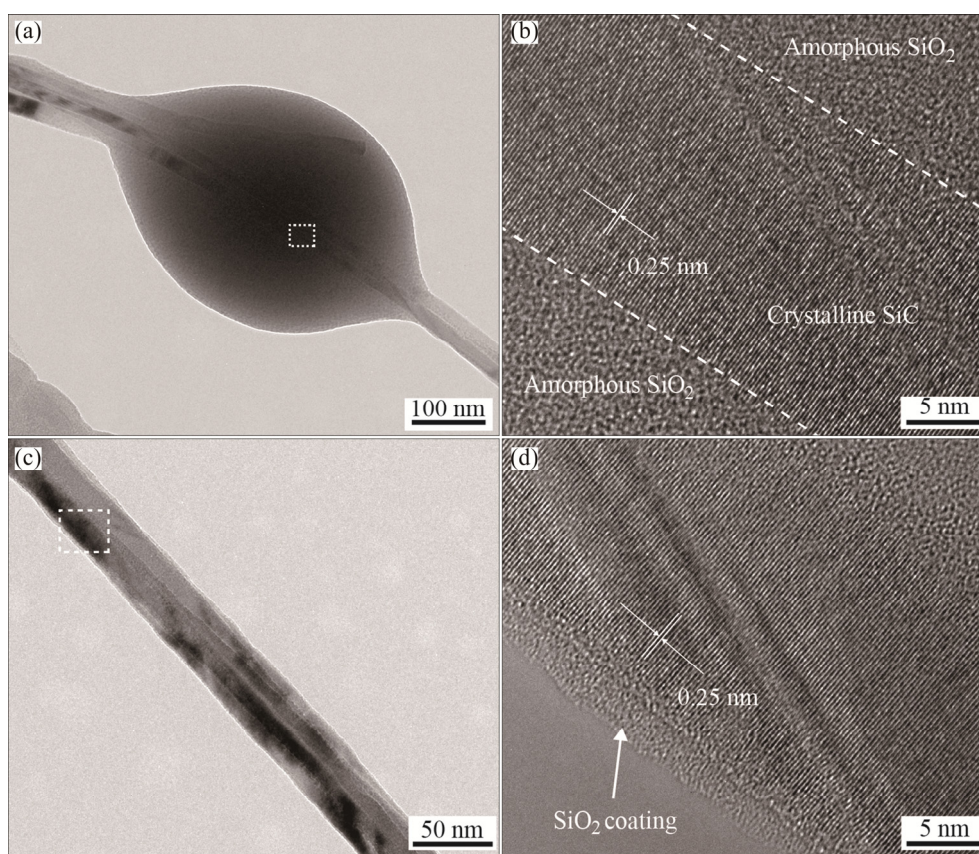
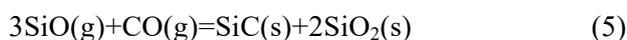


Fig. 6 TEM images of SiC/SiO₂ nanochains synthesized in Ar/CO atmosphere: (a, b) TEM and HRTEM images of bead; (c, d) TEM and HRTEM images of string

fringes in inner part of the bead, and the interplanar spacing (0.25 nm) can be indexed to the (111) plane of SiC, indicating that the inner part of the bead is the single-crystalline SiC. Moreover, no lattice fringes but irregular structures in outer part of the bead are observed so that the outer part of the bead should be amorphous SiO₂. The string (Fig. 6(c)) shows that a core-shell nanowire with a diameter of about 40 nm has a crystalline cubic SiC core, as confirmed by HRTEM image (Fig. 6(d)) which also shows an amorphous SiO₂ shell with a thickness of 3 nm. This kind of SiC/SiO₂ core-shell nanowire has been studied for two decades, and it is believed that the SiO₂ is formed by the reaction between SiO and CO gases, as described in Eq. (5) [33]:



3.2 Growth mechanism of SiC/SiO₂ nanochains

Figure 7(a) shows the standard Gibbs free energy change (ΔG^\ominus) of Reactions (1)–(5). It can be noticed that the ΔG^\ominus values of Reactions (1) and (2) are relatively low, which indicates that both the

silicon and carbon are easy to react with oxygen at high temperature to form the SiO and CO gases, in spite of low oxygen content in the system. In addition, the ΔG^\ominus values of Reactions (3) and (5) are also negative. It seems to suggest that these two reactions may occur easily, leading to the formation of SiC and/or SiO₂. However, no SiO₂ has been detected after reaction in the Ar atmosphere (Figs. 3(a) and 4(a)) in our experiment, presumably because Reaction (5) is not thermodynamically feasible. In order to investigate the influence of vapor pressure of CO gas on the occurrence of Reaction (5), the phase diagrams as the function of $p(\text{CO})$ and temperature are illustrated in Figs. 7(b) and (c). As the SiO and CO gases are both generated in the Ar atmosphere, the vapor pressures of both SiO and CO gases are supposed to be similar (i.e. $p(\text{CO}) \approx p(\text{SiO})$). When the reaction occurs in the Ar atmosphere, the SiO and CO gases from trace oxygen are insufficient to allow the formation of SiO₂ (Fig. 7(b)). By contrast, when the reaction occurs in the Ar/CO atmosphere (about 23 kPa CO in this work), the external CO gas can

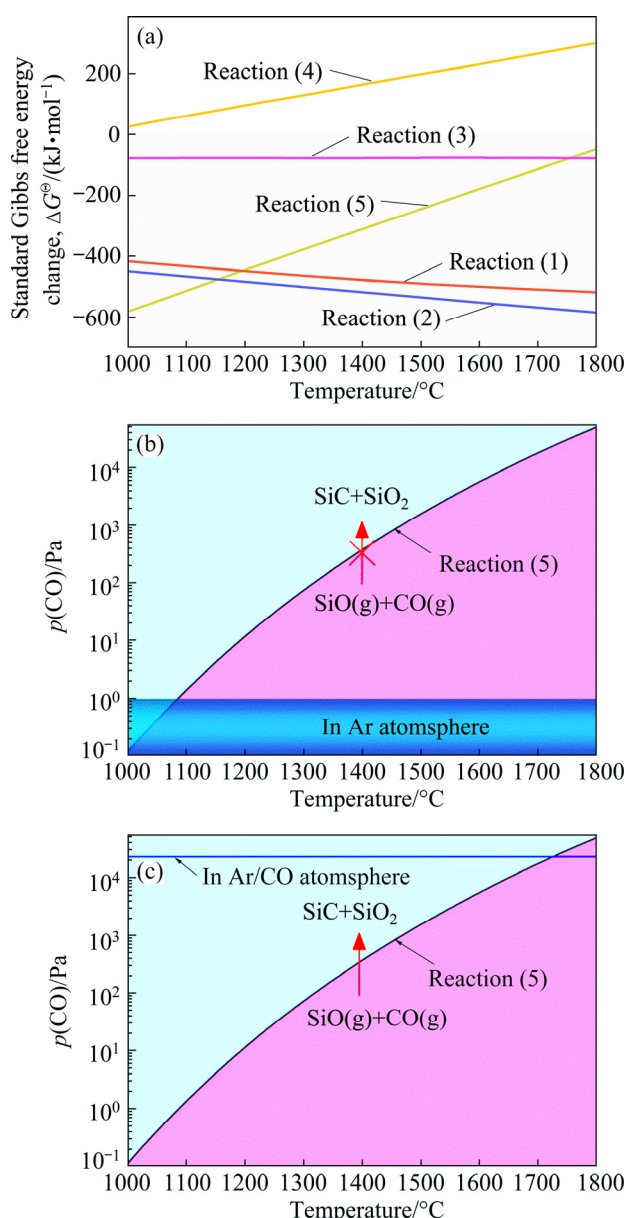


Fig. 7 Standard Gibbs free energy change for Reactions (1)–(5) (a), phase diagrams as functions of temperature and $p(\text{CO})$ in Ar (b) and Ar/CO (c) atmosphere

effectively promote the vapor reaction (Fig. 7(c)), forming a large amount of SiO_2 . Consequently, the formation of SiO_2 during vapor growth process is believed to depend on the vapor pressure of CO.

On the basis of comparative experiments and systematic characterization, the catalyst-free growth mechanism of the SiC/SiO₂ nanochains in the Ar/CO atmosphere can be proposed as follows. Firstly, SiC nanowires are generated from SiO and CO gases, as described in Figs. 8(a–c). Secondly, a high CO partial pressure can make Reaction (5) happen, resulting in the formation of both the SiC and SiO₂ phases as illustrated in Fig. 8(d). The

deposited SiC diffuses to the tips of the nanowires and assists further growth of nanowires along the [111] direction. The SiO₂ phase is absorbed by the SiC nanowires and becomes a molten layer due to good chemical compatibility and wettability between SiO₂ and SiC at a high temperature of 1400 $^\circ\text{C}$. Finally, the SiO₂ melt condenses into the periodic SiO₂ beads on the SiC nanowires during cooling (Figs. 8(e) and (f)). The driving force of wetting is believed to come from the competition between the surface energy of SiO₂ melt and the interfacial energy of SiO₂/SiC. At the synthesis temperature of 1400 $^\circ\text{C}$, the wetting behavior is dominated by the interfacial energy of SiO₂/SiC, and consequently the SiO₂ melt with low viscosity covers the SiC nanowires. As the temperature decreases during cooling, the SiO₂ melt migrates and forms the SiO₂ droplets periodically based on the lowest surface energy principle. These SiO₂ droplets would eventually condense into solid beads on the SiC nanowires (Figs. 6(a) and (b)). At the same time, some SiC nanowires are still coated with SiO₂ film and finally form the SiC/SiO₂ core-shell nanowires (Figs. 6(c) and (d)), because the high viscosity can suppress the migration of SiO₂ on the SiC nanowires during cooling.

3.3 Photoluminescence properties of SiC nanowires and SiC/SiO₂ nanochains

The SiC nanowires are regarded as a good candidate for the application in violet-blue optoelectronic devices, and the SiO₂ is believed to affect the PL properties of SiC nanowires owing to the special electronic structure of the SiC/SiO₂ interface [5,19]. Figure 9(a) shows the photoluminescence (PL) spectra of SiC/SiO₂ nanochains at the excitation wavelength of 250 nm. Four emission peaks at 350, 398, 451 and 467 nm are observed, which are blue-shifted compared to the original 3C–SiC [34]. Similar emission peaks were also reported by WEI et al [9]. Figure 9(b) shows the normalized emission intensity of SiC/SiO₂ nanochains and SiC nanowires. The emission peak of SiC/SiO₂ nanochains shows an obvious blue-shift to 350 nm compared with that of SiC nanowires, which can be ascribed to the influence of SiC/SiO₂ interface interaction and the oxygen discrepancy in the SiO₂ beads [35–37]. This result suggests that the presence of SiO₂ beads can tailor the photoluminescence properties of SiC nanowires.

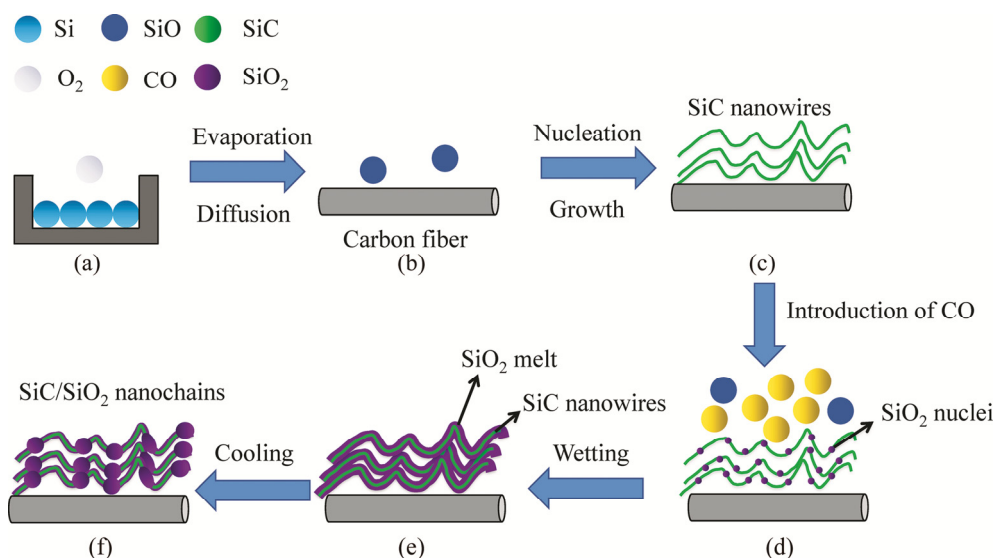


Fig. 8 Growth process of SiC/SiO₂ nanochains

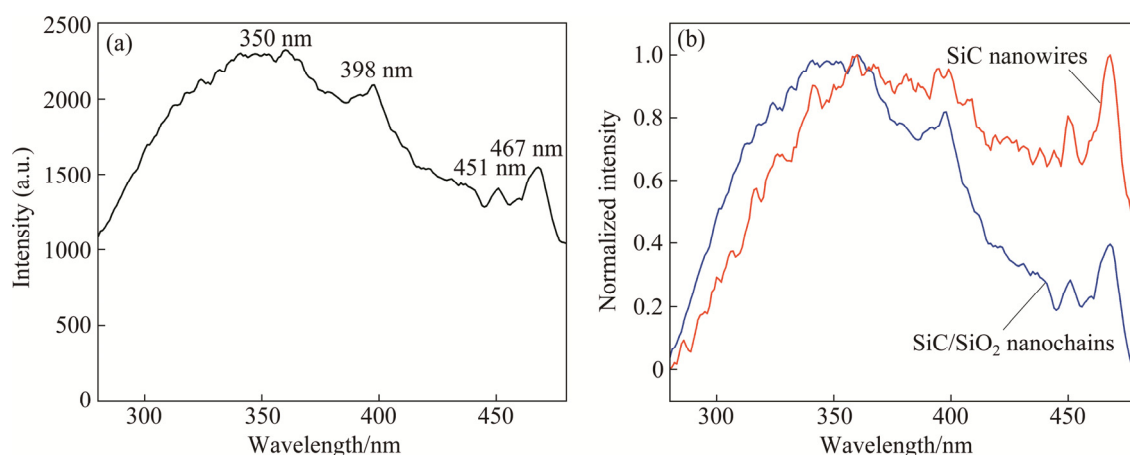


Fig. 9 Photoluminescence spectra of SiC/SiO₂ nanochains (a) and normalized SiC/SiO₂ nanochains and SiC nanowires (b)

4 Conclusions

(1) SiC/SiO₂ nanochains were synthesized by a catalyst-free thermal evaporation method in the Ar/CO atmosphere. The obtained SiC/SiO₂ nanochains consist of crystalline SiC nanowires and amorphous SiO₂ beads.

(2) The comparative experiments revealed that a high CO partial pressure can thermodynamically promote the formation of SiO₂ on SiC nanowires at synthesis temperature, thus leading to the formation of SiC/SiO₂ nanochains during cooling.

(3) The SiC/SiO₂ nanochains showed an obvious blue-shift to 350 nm compared with SiC nanowires, which can provide a way to tune the

optoelectronic behavior of SiC-based functional device.

References

- [1] ZATKO B, HRUBCIN L, SAGATOVA A, OSVALD J, BOHACEK P, ZAPRAZNY Z, SEDLACKOVA K, SEKACOVA M, DUBECKY F, SKURATOV V A, KORYTAR D, NECAS V. Schottky barrier detectors based on high quality 4H-SiC semiconductor: Electrical and detection properties [J]. Applied Surface Science, 2018, 461: 276–280.
- [2] SAVINO R, CRISCUOLO L, DI MARTINO G D, MUNGIGUERRA S. Aero-thermo-chemical characterization of ultra-high-temperature ceramics for aerospace applications [J]. Journal of the European Ceramic Society, 2018, 38: 2937–2953.
- [3] ZENG K H, MA Q S, GU X Y. Effects of SiC interfacial

- coating on mechanical properties of carbon fiber needled felt reinforced sol-derived Al_2O_3 composites [J]. Transactions of Nonferrous Metals Society of China, 2020, 30: 463–471.
- [4] RAN L P, RAO F, PENG K, YIN H, YI M Z. Preparation and properties of C/C– ZrB_2 –SiC composites by high-solid-loading slurry impregnation and polymer infiltration and pyrolysis (PIP) [J]. Transactions of Nonferrous Metals Society of China, 2019, 29: 2141–2150.
- [5] FAN J Y, WU X L, CHU P K. Low-dimensional SiC nanostructures: Fabrication, luminescence, and electrical properties [J]. Progress in Materials Science, 2006, 51: 983–1031.
- [6] FENG W, MA J T, YANG W Y. Precise control on the growth of SiC nanowires [J]. Cryst Eng Comm, 2012, 14: 1210–1212.
- [7] LIU S L, LIU H T, HUANG Z H, FANG M H, LIU Y G, WU X W. Synthesis of beta-SiC nanowires via a facile CVD method and their photoluminescence properties [J]. RSC Advances, 2016, 6: 24267–24272.
- [8] GE Y C, LIU Y Q, WU S, HUANG W Q, MAO P L, YI M Z. Characterization of SiC nanowires prepared on C/C composite without catalyst by CVD [J]. Transactions of Nonferrous Metals Society of China, 2015, 25: 3258–3264.
- [9] WEI G D, QIN W P, ZHENG K Z, ZHANG D S, SUN J B, LIN J J, KIM R J, WANG G F, ZHU P F, WANG L L. Synthesis and properties of SiC/SiO₂ nanochain heterojunctions by microwave method [J]. Crystal Growth & Design, 2009, 9: 1431–1435.
- [10] KUDRENKO E, RODDATIS V, ZHOKHOV A, ZVERKOVA I, KHODOS I, EMELCHENKO G. Morphology of SiC nanowires grown on the surface of carbon fibers [J]. RSC Advances, 2012, 2: 4913–4919.
- [11] XIN L P, SHI Q, CHEN J J, TANG W H, WANG N Y, LIU Y, LIN Y X. Morphological evolution of one-dimensional SiC nanomaterials controlled by sol–gel carbothermal reduction [J]. Materials Characterization, 2012, 65: 55–61.
- [12] LI Z J, GAO W D, MENG A, GENG Z D, WAN L B. Effects of Fe and Ni on the yield and morphology of the 1D SiC nanostructures prepared by chemical vapor reaction [J]. Journal of Crystal Growth, 2008, 310: 4401–4406.
- [13] DAI J X, SHA J J, ZHANG Z Q, SHAO J Q, ZU Y F, LEI M K. Catalyst-free growth of multi-shaped SiC nanofibers on carbon fibers at elevated temperatures [J]. Ceramics International, 2017, 43: 17057–17063.
- [14] DAI J X, SHA J J, ZU Y F, SHAO J Q, LEI M K, FLAUDER S, LANGHOF N, KRENKEL W. Synthesis and growth mechanism of SiC nanofibers on carbon fabrics [J]. Cryst Eng Comm, 2017, 19: 1279–1285.
- [15] HOU H L, WANG L, GAO F M, WEI G D, ZHENG J J, CHENG X M, TANG B, YANG W Y. Mass production of SiC/SiO_x nanochain heterojunctions with high purities [J]. Cryst Eng Comm, 2013, 15: 2986–2991.
- [16] ZHONG B, KONG L Q, ZHANG B, YU Y L, XIA L. Fabrication of novel hydrophobic SiC/SiO₂ bead-string like core-shell nanochains via a facile catalyst/template-free thermal chemical vapor deposition process [J]. Materials Chemistry and Physics, 2018, 217: 111–116.
- [17] LI W, JIA Q L, LIU X H, ZHANG J. Large scale synthesis and photoluminescence properties of necklace-like SiC/SiO_x heterojunctions via a molten salt mediated vapor reaction technique [J]. Ceramics International, 2017, 43: 2950–2955.
- [18] DAI J X, SHA J J, ZHANG Z F, SHAO J Q, ZU Y F, LEI M K. Synthesis of novel hierarchical SiC–SiO₂ heterostructures via a catalyst free method [J]. Cryst Eng Comm, 2017, 19: 6540–6546.
- [19] FAN J Y, CHU P K. Silicon carbide nanostructures: Fabrication, structure, and properties [M]. Heidelberg: Springer, 2014.
- [20] LI W, JIA Q L, YANG D Y, LIU X H. Tunable synthesis of SiC/SiO₂ heterojunctions via temperature modulation [J]. Materials, 2018, 11: 766–776.
- [21] LI Z J, ZHAO J, ZHANG M, XIA J Y, MENG A. SiC nanowires with thickness-controlled SiO₂ shells: Fabrication, mechanism, reaction kinetics and photoluminescence properties [J]. Nano Research, 2015, 7: 462–472.
- [22] RYU Y, TAK Y, YONG K. Direct growth of core-shell SiC–SiO₂ nanowires and field emission characteristics [J]. Nanotechnology, 2005, 16: 370–374.
- [23] CHU Y H, JING S Y, YU X, ZHAO Y L. High-temperature plateau-rayleigh growth of beaded SiC/SiO₂ nanochain heterostructures [J]. Crystal Growth & Design, 2018, 18: 2941–2947.
- [24] WU F, MYUNG Y, BANERJEE P. Rayleigh instability driven nodular Cu₂O nanowires via carbothermal reduction of CuO nanowires [J]. Crystal Growth & Design, 2014, 15: 1588–1595.
- [25] GORUP L, SOUZA NETO F, KUBO A, SANTOS SOUZA J A, FERNANDES SCAPPATICCI R, LOPES G, MONTEIRO D, BARROS BARBOSA D, CAMARGO E. Recent advances in complex functional materials [M]. Heidelberg: Springer, 2017.
- [26] SUBANNAJUI K, RAMGIR N S, GRIMM R, MICHIELS R, YANG Y, MULLER S, ZACHARIAS M. ZnO Nanowire growth: A deeper understanding based on simulations and controlled oxygen experiments [J]. Crystal Growth & Design, 2010, 10: 1585–1589.
- [27] RAY S, DAS D, BARUA A K. Infrared vibrational spectra of hydrogenated amorphous silicon carbide thin films prepared by glow discharge [J]. Solar Energy Materials, 1987, 15: 45–57.
- [28] MACDONALD S A, SCHARDT C R, MASIELLO D J, SIMMONS J H. Dispersion analysis of FTIR reflection measurements in silicate glasses [J]. Journal of Non-Crystalline Solids, 2000, 275: 72–82.
- [29] CHU Y H, JING S Y, CHEN J K. In situ synthesis of homogeneously dispersed SiC nanowires in reaction sintered silicon-based ceramic powders [J]. Ceramics International, 2018, 44: 6681–6685.
- [30] KHOLMANOV I N, KHARLAMOV A, BARBORINI E, LENARDI C, LI BASSI A, BOTTANI C E, DUCATI C, MAFFI S, KIRILLOVA N V, MILANI P. A simple method for the synthesis of silicon carbide nanorods [J]. Journal of Nanoscience and Nanotechnology, 2002, 2: 453–456.
- [31] DAI J J, SHA J J, ZHANG Z F, WANG Y, KRENKEL W. Synthesis of high crystalline beta SiC nanowires on a large scale without catalyst [J]. Ceramics International, 2015, 41: 9637–9641.

- [32] HUANG Z H, LIU H T, CHEN K, FANG M H, HUANG J T, LIU S Y, HUANG S F, LIU Y G, WU X W. Synthesis and formation mechanism of twinned SiC nanowires made by a catalyst-free thermal chemical vapour deposition method [J]. RSC Advances, 2014, 4: 18360–18364.
- [33] LI B S, WU R B, PAN Y, WU L L, YANG G Y, CHEN J J, ZHU Q M. Simultaneous growth of SiC nanowires, SiC nanotubes, and SiC/SiO₂ core-shell nanocables [J]. Journal of Alloys and Compounds, 2008, 462: 446–451.
- [34] CHIU S C, LI Y Y. SiC nanowires in large quantities: Synthesis, band gap characterization, and photoluminescence properties [J]. Journal of Crystal Growth, 2009, 311: 1036–1041.
- [35] WEI G D, QIN W P, ZHU P F, KIM R J, WANG G F, ZHANG D S, ZHENG K Z, WANG L L. Large-scale synthesis and photoluminescence properties of aligned multicore SiC–SiO₂ nanocables [J]. Journal of Nanoscience and Nanotechnology, 2010, 10: 1964–1968.
- [36] LIANG C, MENG G, ZHANG L, WU Y, CUI Z. Large-scale synthesis of β -SiC nanowires by using mesoporous silica embedded with Fe nanoparticles [J]. Chemical Physics Letters, 2000, 329: 323–328.
- [37] CAI K F, ZHANG A X, YIN J L, WANG H F, YUAN X H. Preparation, characterization and photoluminescence properties of ultra long SiC/SiO_x nanocables [J]. Applied Physics A, 2008, 91: 579–584.

Ar/CO 气氛下无催化剂热蒸发法制备 SiC/SiO₂ 纳米链及其生长机理

谢翔旻¹, 苏哲安¹, 黄东², 杨程¹, 王亚峰¹, 姜定宇¹, 黄启忠¹

1. 中南大学 轻质高强结构材料国防科技重点实验室, 长沙 410083;
2. 湖南东映碳材料科技有限公司 湖南省高性能沥青基碳材料工程研究中心, 长沙 410205

摘要: 在 Ar/CO 气氛中采用无催化剂热蒸发法在碳纤维基体表面制备 SiC/SiO₂ 纳米链。XRD、FT-IR、SEM 和 TEM 结果表明: 所制备的 SiC/SiO₂ 纳米链由单晶结构 SiC 纳米线和无定形结构 SiO₂ 球组成。CO 的引入能促进形成 SiO₂, 从而在冷却过程中形成 SiC/SiO₂ 纳米链。此外, 光致发光光谱分析结果表明, SiC/SiO₂ 纳米链在约 350 nm 处显示出一个较宽的发射峰, 主要是由于 SiO₂ 球中的氧偏差以及 SiC/SiO₂ 的界面效应。本研究能为一维碳化硅基材料气相生长的研究提供指导。

关键词: 合成; 生长机理; SiC/SiO₂ 纳米链; 热蒸发法; 一氧化碳; 光致发光性能

(Edited by Wei-ping CHEN)